

Article

Shkatulkalite, a Rare Mineral from the Lovozero Massif, Kola Peninsula: A Re-Investigation

Andrey A. Zolotarev Jr. ¹, Ekaterina A. Selivanova ², Sergey V. Krivovichev ^{1,3,*}, Yevgeny E. Savchenko ² , Taras L. Panikorovskii ^{1,3} , Lyudmila M. Lyalina ², Leonid A. Pautov ⁴ and Victor N. Yakovenchuk ^{2,3}

¹ Department of Crystallography, Institute of Earth Sciences, Saint Petersburg State University, University Emb. 7/9, 199034 St. Petersburg, Russia; aazolotarev@gmail.com (A.A.Z.J.); rotor_vlg@list.ru (T.L.P.)

² Geological Institute, Kola Science Centre, Russian Academy of Sciences, Fersmana 14, 184209 Apatity, Russia; selivanova@geoksc.apatity.ru (E.A.S.); evsav@geoksc.apatity.ru (Y.E.S.); lyalinalyudmila71@mail.ru (L.M.L.); yakovenchuk@geoksc.apatity.ru (V.N.Y.)

³ Nanomaterials Research Centre, Kola Science Centre, Russian Academy of Sciences, Fersmana 14, 184209 Apatity, Russia

⁴ Fersman Mineralogical Museum, Russian Academy of Sciences, Leninskiy Av. 18/2, 115162 Moscow, Russia; pla58@mail.ru

* Correspondence: s.krivovichev@spbu.ru or krivovichev@admksk.apatity.ru; Tel.: +7-815-557-53-50

Received: 18 May 2018; Accepted: 12 July 2018; Published: 18 July 2018



Abstract: The crystal structure of shkatulkalite has been solved from the crystal from the Lovozero alkaline massif, Kola Peninsula, Russia. The mineral is monoclinic, $P2/m$, $a = 5.4638(19)$, $b = 7.161(3)$, $c = 15.573(6)$ Å, $\beta = 95.750(9)^\circ$, $V = 606.3(4)$ Å³, $R_1 = 0.080$ for 1551 unique observed reflections. The crystal structure is based upon the *HOH* blocks consisting of one octahedral (*O*) sheet sandwiched between two heteropolyhedral (*H*) sheets. The blocks are parallel to the (001) plane and are separated from each other by the interlayer space occupied by *Na*1 atoms and H₂O groups. The *Na*2, *Na*3, and *Ti* sites are located within the *O* sheet. The general formula of shkatulkalite can be written as $\text{Na}_5(\text{Nb}_{1-x}\text{Ti}_x)_2(\text{Ti}_{1-y}\text{Mn}^{2+}_y)[\text{Si}_2\text{O}_7]_2\text{O}_2(\text{OH})_2 \cdot n\text{H}_2\text{O}$, where $x + y = 0.5$ and $x \approx y \approx 0.25$ for the sample studied. Shkatulkalite belongs to the seidozerite supergroup and is a member of the lamprophyllite group. The species most closely related to shkatulkalite are vuonnemite and epistolite. The close structural relations and the reported observations of pseudomorphs of shkatulkalite after vuonnemite suggest that, at least in some environments, shkatulkalite may form as a transformation mineral species.

Keywords: shkatulkalite; titanosilicate; crystal structure; Kola Peninsula; Lovozero alkaline massif; transformation mineral species; vuonnemite; titanium; niobium

1. Introduction

Titanosilicates constitute an important group of minerals that have found many applications as materials, including ion-exchange, sorption, catalysis, optics, biocide technologies, etc. [1–5]. Of particular interest are layered titanosilicates of the seidozerite supergroup that currently contains more than forty-five mineral species [6] with several new minerals described very recently [7–13]. These species occur mainly in alkaline massifs such as those in Kola Peninsula, Russia, above the Polar circle. Belov and Organova [14] were the first who considered the crystal chemistry of several minerals of the current murmanite group of seidozerite supergroup [6]. Belov [15] and Pyatenko et al. [16] made further generalizations and called minerals with a “seidozerite block” (=TS block, [17]) and astrophyllite-group minerals titanosilicate analogues of micas. The modular approach to these minerals

has been developed by Egorov-Tismenko and Sokolova [18,19], who described a homologous series of Ti-analogues of micas, and Ferraris [20–22], who named those minerals heterophyllosilicates and described them as members of a single polysomatic series. Sokolova [17] quantitatively divided TS-block minerals into four groups based on the content of Ti, structural topology and stereochemistry of the TS block.

Shkatulkalite, $\text{Na}_{10}\text{MnTi}_3\text{Nb}_3(\text{Si}_2\text{O}_7)_6(\text{OH})_2\text{F}\cdot 12\text{H}_2\text{O}$, was described by Menshikov et al. [23] from the pegmatite “Shkatulka” of the Lovozero alkaline massif, Kola Peninsula, Russia. The mineral was considered to be a Ti–Nb–sorosilicate of the “epistolite group” (now considered a part of the lamprophyllite group [24]). In their review on the seidozerite-supergroup minerals, Sokolova and Cámara [6] pointed out that shkatulkalite is a potential member of the supergroup, but the final assignment of the mineral to a particular group remained unclear, due to the fact that its crystal structure was unknown until now. Menshikov et al. [23] established that the mineral is monoclinic, $a = 5.468(9)$, $b = 7.18(1)$, $c = 31.1(1)$ Å, $\beta = 94.0(2)^\circ$, $V = 1218(8)$ Å³, $Z = 1$, and commented on the proximity of the a and b parameters of shkatulkalite to those typical for other known Ti and Nb sorosilicates. On the basis of systematic absences, the space groups Pm , $P2$, $P2/m$ were proposed as possible for the mineral. However, due to the poor quality of single-crystal X-ray diffraction data, the structure of the mineral could not be solved at the time. Németh et al. [25] investigated syntactic intergrowths of epistolite, murmanite and shkatulkalite using transmission electron microscopy (TEM) and selected-area electron diffraction (SAED), and reported on the absence of the $l = 2n + 1$ reflections for the latter mineral, pointing out that its c parameter is halved with respect to the value of 31.1 Å reported by Menshikov et al. [23]. Later, shkatulkalite was described in nepheline syenites of the alkaline sill of St. Amable, Quebec, Canada [26], as forming prismatic crystals and radial intergrowth of crystals in small miarolitic voids as well as in a hydrothermal cavity in the southeastern part of the Demix quarry. The authors [26] noted that the shkatulkalite is visually indistinguishable from vuonnemite and epistolite found in the same voids. At the same time, Menshikov et al. [23] pointed out that shkatulkalite sometimes forms pseudomorphs after vuonnemite and thus can be considered as a transformation mineral species [27,28], that is, mineral species that forms as a result of a secondary transformation of a primary proto-phase. However, this hypothesis could not be confirmed until the crystal structure of the mineral is solved.

The aim of the present paper is to report the results of crystal-structure determination of shkatulkaite and to re-consider its status as both seidozerite-supergroup mineral and transformation mineral species.

2. Materials and Methods

2.1. Occurrence

The ultra-agpaitic pegmatite body “Shkatulka” located in the western part of the Alluaiv mountain of the Lovozero alkaline massif was discovered by underground excavations in 1990 [29]. Shkatulkalite was found in the marginal zone of the ussingite core of the pegmatite and in the adjacent aegirine zone [23]. The mineral was represented by three morphological varieties: (1) rectangular plates and tabular crystals; (2) aggregates of nacreous mica-like flakes; (3) partial pseudomorphs after vuonnemite. The first variety has the best quality of the material and was used as a holotype sample. In the present work we used material provided by the Museum of the Geological Institute of the Kola Science Center of the Russian Academy of Sciences, sample No. GIM 5968/2-1. It turned out that, in addition to the three types of shkatulkalite identified previously by Menshikov et al. [23], there is also fourth, which is not visually different from vuonnemite and only sometimes has a slightly lighter tone. Some areas of matte from the white or slightly yellowish to cream-colored large vuonnemite plates turned out to be shkatulkalite, and this material proved to be suitable for the single-crystal X-ray diffraction studies. The main difficulty of studying this material was in the preparation of samples for microprobe analysis, due to the poor polishability of its crystals.

2.2. Chemical Composition

The chemical composition of shkatulkalite was studied in three independent laboratories. Initially, the analyzes were performed at the Resource Center “Geomodel” of St. Petersburg State University using the AzTec Energy 350 energy dispersive attachment to the Hitachi S-3400N scanning electron microscope (Hitachi, Tokyo, Japan), operating at 20 kV, 20–30 nA, with a 5 μm beam diameter. The standards used were: lorenzenite (Na), periclase (Mg), diopside (Ca), quartz (Si), microcline (K), barite (Ba), rutile (Ti), rhodonite (Mn), corundum (Al), celestine (Sr), hematite (Fe), and Nb (Nb). Alternatively the chemical composition of shkatulkalite also was determined by the wavelength-dispersive spectrometry on a Cameca MS-46 electron microprobe (Geological Institute, Kola Science Centre, Russian Academy of Sciences, Apatity) operating at 22 kV (for Sr at 30 kV), 20–40 nA. Due to the easy dehydration of the mineral in a vacuum, and its deterioration under an electron beam, the measurements were carried out with a defocused beam up to 20 μm , while manually moving the sample. The standards used were: lorenzenite (NaK α , TiK α), wollastonite (CaK α , SiK α), orthoclase (KK α), synthetic MnCO₃ (MnK α), Y₃Al₅O₁₂ (AlK α), hematite (FeK α), apatite (PK α) and Nb (NbL α). The fluorine was determined using an Xflash-5010 Bruker Nano GmbH energy dispersive X-ray spectrometer (Bruker, Bremen, Germany) mounted on a scanning electron microscope LEO-1450 at 20 kV and 0.5 nA. A non-standard procedure for the P/B-ZAF method of Quantax-200 was used. Table 1 provides the summary of analytical results.

Table 1. Chemical composition of shkatulkalite ¹.

Component	1		2		3		4	
	Mean	Range	Mean	Range	Mean	Range	Mean	Range
Chemical Composition in wt %								
Na ₂ O	13.90	13.25–14.30	14.69	13.75–15.39	16.14	15.60–16.84	16.15	14.70–17.57
CaO	0.43	0.28–0.61	0.50	0.43–0.56	0.44	0.40–0.52	0.55	0.49–0.62
SrO	2.07	1.59–2.51	1.03	0.98–1.07	0.46	0.26–0.60	1.01	0.65–1.85
MnO	1.58	1.14–1.90	1.86	1.79–1.91	1.70	1.54–1.81	1.92	1.70–2.28
K ₂ O	0.27	0.23–0.33	0.18	0.17–0.22	-	-	0.25	0.20–0.41
BaO	1.08	0.82–1.38	n.d.	n.d.	-	-	0.06	0.01–0.29
FeO	n.d.	n.d.	0.08	0.06–0.10	-	-	0.12	0.02–0.19
Fe ₂ O ₃	-	-	-	-	0.07	0.05–0.08	-	-
Al ₂ O ₃	n.d.	n.d.	0.13	0.11–0.16	0.24	0.21–0.28	0.16	0.08–0.62
SiO ₂	31.52	31.24–32.07	32.24	31.59–32.60	35.70	35.58–35.84	32.71	31.65–33.74
TiO ₂	10.68	10.04–11.41	11.59	11.51–11.64	11.12	11.03–11.23	10.87	10.60–11.19
Nb ₂ O ₅	22.72	21.49–23.92	22.55	21.89–23.05	21.93	21.72–22.22	22.65	21.30–24.14
P ₂ O ₅	n.d.	n.d.	0.32	0.26–0.38	-	-	0.43	0.21–0.98
F	not measured		0.96	0.77–1.17	0.94	-	1.51	0.77–1.83
H ₂ O	15.75 ²	-	14.67 ²	-	11.66 ²	-	12.25	-
-O=F ₂	-	-	0.40	-	0.40	-	0.64	-
Total	100.00	-	100.00	-	100.00	-	100.00	-
Chemical Composition in Atoms per Formula Unit (apfu)								
Basis	Si = 4		Si + Al = 4		Si + Al + Fe = 4		Si + Al + Fe = 4	
Na	3.42	-	3.52	-	3.47	-	3.80	-
Ca	0.06	-	0.07	-	0.05	-	0.07	-
Sr	0.15	-	0.07	-	0.03	-	0.07	-
Mn	0.17	-	0.19	-	0.16	-	0.20	-
K	0.06	-	0.03	-	-	-	0.04	-
Ba	0.05	-	-	-	-	-	-	-
Fe	-	-	0.01	-	0.01	-	0.01	-
Al	-	-	0.02	-	0.03	-	0.02	-
Si	4.00	-	3.98	-	3.96	-	3.97	-
Ti	1.02	-	1.08	-	0.93	-	0.99	-
Nb	1.30	-	1.26	-	1.10	-	1.24	-
P	-	-	0.03	-	-	-	0.04	-
F	-	-	0.37	-	0.33	-	0.58	-
H	13.34	-	12.09	-	8.64	-	9.91	-

¹ 1–3—this work (1—Hitachi S-3400N; 2—Cameca MS-46, 3—JEOL 733); 4—Menshikov et al. [23]; ² calculated by difference to 100%.

The chemical composition of shkatulkalite also was studied by the wavelength-dispersive spectrometry on a JEOL Superprobe 733 electron microprobe (Fersman Geological Museum, Russian Academy of Sciences, Moscow) operating at 15 kV and 15 nA. Due to the easy dehydration of the mineral in a vacuum and its deterioration under an electron beam, the measurements were carried out with a defocused beam up to 20 μm . The standards used were: chkalovite ($\text{NaK}\alpha$), diopside ($\text{CaK}\alpha$), microcline ($\text{KK}\alpha$), tephroite ($\text{MnK}\alpha$), almandine ($\text{FeK}\alpha$, $\text{SiK}\alpha$, $\text{AlK}\alpha$), synthetic AlPO_4 ($\text{PK}\alpha$), synthetic BaSO_4 ($\text{BaK}\alpha$), synthetic SrTiO_3 ($\text{SrK}\alpha$, $\text{TiK}\alpha$), fluorphlogopite ($\text{FK}\alpha$), and synthetic $\text{Cs}_2\text{Nb}_4\text{O}_{11}$ for Nb ($\text{NbL}\alpha$). It was observed that shkatulkalite contains rutile inclusions oriented parallel to the (001) plane (Figure 1a). Shkatulkalite shows significant variations of different elements (Figure 1b–f). No elements other than those mentioned above were detected.

The resulting empirical formulae obtained in our study can be written as $(\text{Na}_{3.42}\text{Sr}_{0.15}\text{Ca}_{0.06}\text{K}_{0.06}\text{Ba}_{0.05})_{3.84}(\text{Nb}_{1.30}\text{Ti}_{1.02}\text{Mn}^{2+}_{0.17})_{2.49}(\text{Si}_2\text{O}_7)_2\text{O}_{0.47}(\text{OH})_2 \cdot 5.67\text{H}_2\text{O}$ (for sample 1), $(\text{Na}_{3.52}\text{Sr}_{0.07}\text{Ca}_{0.07}\text{K}_{0.03})_{3.69}(\text{Nb}_{1.26}\text{Ti}_{1.08}\text{Mn}^{2+}_{0.19})_{2.53}(\text{Si}_{1.99}\text{Al}_{0.01}\text{O}_7)_2[(\text{OH})_{1.63}\text{F}_{0.37}]\text{O}_{0.44} \cdot 5.23\text{H}_2\text{O}$ (for sample 2) and $(\text{Na}_{3.47}\text{Sr}_{0.03}\text{Ca}_{0.05})_{3.69}(\text{Nb}_{1.10}\text{Ti}_{0.93}\text{Mn}^{2+}_{0.16})_{2.53}(\text{Si}_{1.98}\text{Al}_{0.02}\text{O}_7)_2[(\text{OH})_{0.80}\text{F}_{0.33}]_{1.13} \cdot 3.49\text{H}_2\text{O}$ (for sample 3). These results are in very general agreement with the results of the crystal-structure study discussed below, taken into account the high instability of the mineral under electron beam.

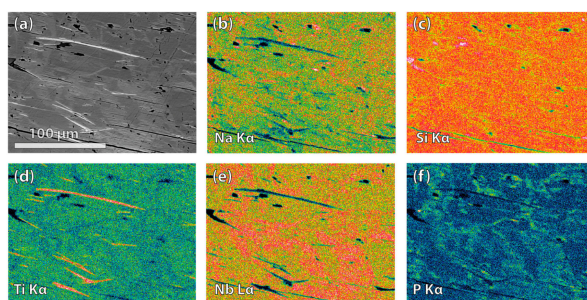


Figure 1. Backscattered electron image of shkatulkalite crystal (a) and X-ray distribution maps for Na K α (b); Si K α (c); Ti K α (d); Nb L α (e); P K α (f) radiation.

2.3. Single-Crystal X-ray Diffraction

Single-crystal X-ray diffraction study of shkatulkalite was performed at the Resource Center “X-ray Diffraction Methods” of St. Petersburg State University using Bruker Kappa APEX DUO diffractometer operated at 45 kV and 0.6 mA and equipped with a CCD (charge-coupled device) area detector. The study was done by means of a monochromatic MoK α X-radiation ($\lambda = 0.71073 \text{ \AA}$), frame widths of 0.5° in ω and 30 s counting time for each frame. The intensity data were reduced and corrected for Lorentz, polarization and background effects using the Bruker software APEX2 [30]. A semiempirical absorption-correction based upon the intensities of equivalent reflections was applied (SADABS [31]). The unit-cell parameters were refined by least square techniques using 4463 reflections. In general, the unit-cell parameters obtained in this study are in agreement with those reported by Menshikov et al. [23], but with the c parameter halved (15.573 instead of 31.1 \AA), thus confirming the observations by Németh et al. [25] (see above). The structure was solved and refined in space group $P2/m$ to $R_1 = 0.080$ ($wR_2 = 0.195$) for 1378 unique observed reflections using ShelX program package [32] within the Olex2 shell [33]. Crystal data, data collection and structure refinement details are given in Table 2; atom coordinates, occupancies and displacement parameters in Tables 3 and 4, selected interatomic distances in Table 5. Occupancies of the cation sites were calculated from the experimental site-scattering factors taking into account empirical formulae. Table 6 provides the results of bond-valence analysis with bond-valence parameters taken from [34].

Table 2. Crystal data and structure refinement for shkatulkalite.

Crystal System	Monoclinic
Space group	<i>P2/m</i>
<i>a</i> , Å	5.4638(19)
<i>b</i> , Å	7.161(3)
<i>c</i> , Å	15.573(6)
β , °	95.750(9)
<i>V</i> , Å ³	606.3(4)
<i>Z</i>	1
ρ_{calc} , g/cm ³	2.370
μ , mm ⁻¹	1.988
Crystal dimensions, mm	0.13 × 0.10 × 0.05
<i>F</i> (000)	418.0
Radiation	MoK α (λ = 0.71073)
2 Θ range, deg.	2.63–56.00
Index ranges	$-7 \leq h \leq 7$, $-8 \leq k \leq 9$, $-17 \leq l \leq 20$
Reflections collected	4463
Independent reflections	1551 [$R_{\text{int}} = 0.0550$, $R_{\text{sigma}} = 0.0652$]
Data/restraints/parameters	1551/0/126
GOF (goodness-of-fit)	1.202
Final <i>R</i> indexes [$I \geq 2\sigma(I)$]	$R_1 = 0.0801$, $wR_2 = 0.1947$
Final <i>R</i> indexes [all data]	$R_1 = 0.0892$, $wR_2 = 0.1997$
Largest diff. peak/hole/ $e^{-}\text{\AA}^{-3}$	1.88/−1.16

Table 3. Atomic coordinates, experimental and calculated site-scattering factors (SSF_{exp} and SSF_{calc} , respectively) and isotropic displacement parameters (\AA^2) for shkatulkalite.

Atom	<i>x</i>	<i>y</i>	<i>z</i>	Occupancy	SSF_{exp} [e^{-}]	SSF_{calc} [e^{-}]	U_{eq}
<i>Nb</i>	0.5901(2)	0	0.30252(7)	Nb _{0.75} Ti _{0.25}	36.3(7)	36.25	0.0102(4)
<i>Ti</i>	0	1/2	1/2	Ti _{0.77} Mn _{0.20} □ _{0.03}	22.0(4)	22.00	0.027(1)
<i>Si</i>	0.0947(3)	0.7115(3)	0.3227(1)	Si	14.0(2)	14.00	0.0117(6)
<i>Na1</i>	0.5803(8)	1/2	0.2572(7)	Na _{0.60} □ _{0.25} Sr _{0.07} Ba _{0.06} K _{0.02}	13.0(3)	13.00	0.079(4)
<i>Na2</i>	0.5	0.7437(6)	1/2	Na _{0.87} Mn _{0.07} Ca _{0.06}	12.5(2)	12.52	0.019(2)
<i>Na3</i>	0	0	1/2	Na	11.0(3)	11.00	0.018(1)
<i>O1</i>	0.331(1)	0.8064(9)	0.2873(4)	O	8.0(1)	8.00	0.024(1)
<i>O2</i>	0.085(2)	1/2	0.2832(6)	O	8.0(1)	8.00	0.021(2)
<i>O3</i>	0.841(1)	0.8087(9)	0.2841(4)	O	8.0(1)	8.00	0.023(1)
<i>O4</i>	0.1206(9)	0.7024(7)	0.4268(3)	O	8.0(1)	8.00	0.013(1)
<i>O5</i>	0.627(1)	0	0.4167(5)	O	8.0(1)	8.00	0.017(2)
<i>X6</i>	0.684(1)	1/2	0.4282(5)	(OH) _{0.82} F _{0.18}	8.0(1)	8.18	0.018(2)
<i>O_w1</i>	0.542(2)	0	0.1551(7)	(H ₂ O) _{0.94}	7.5(3)	7.52	0.040(3)
<i>O_w2</i>	0.536(7)	0.410(5)	0.134(2)	(H ₂ O) _{0.37}	2.7(2)	2.96	0.09(1)
<i>O_w3</i>	0.044(3)	0	0.158(1)	(H ₂ O) _{0.92}	7.4(4)	7.36	0.085(8)
<i>O_w4</i>	1/2	1/2	0	(H ₂ O) _{0.19}	1.5(5)	1.52	0.04(3)
<i>O_w5</i>	0.771(8)	1/2	0.001(3)	(H ₂ O) _{0.24}	1.9(3)	1.92	0.04(2)
<i>O_w6</i>	0.019(5)	0.380(4)	0.058(2)	(H ₂ O) _{0.14}	1.1(1)	1.12	0.003(9)
<i>O_w7</i>	0	0.259(7)	0	(H ₂ O) _{0.31}	2.5(4)	2.48	0.06(2)
<i>O_w8</i>	0.65(1)	0	0.001(5)	(H ₂ O) _{0.25}	2.0(4)	2.00	0.09(3)

Table 4. Anisotropic displacement atom parameters for shkatulkalite (Å²).

Atom	U^{11}	U^{22}	U^{33}	U^{23}	U^{13}	U^{12}
Nb	0.0033(5)	0.0060(6)	0.0213(7)	0	0.0004(3)	0
Ti	0.044(2)	0.005(2)	0.038(2)	0	0.029(2)	0
Si	0.0078(9)	0.006(1)	0.021(1)	−0.0003(7)	0.0007(7)	0.0008(7)
Na1	0.012(2)	0.006(3)	0.22(1)	0	0.027(3)	0
Na2	0.009(2)	0.016(2)	0.032(3)	0	−0.004(1)	0
Na3	0.010(3)	0.019(3)	0.024(3)	0	−0.006(2)	0
O1	0.018(3)	0.025(3)	0.032(3)	−0.004(3)	0.008(2)	−0.014(2)
O2	0.029(4)	0.005(4)	0.029(5)	0	0.001(3)	0
O3	0.020(3)	0.022(3)	0.028(3)	0	0.001(2)	0.012(2)
O4	0.012(2)	0.009(3)	0.020(3)	−0.001(2)	0.002(2)	−0.001(2)
O5	0.011(3)	0.016(4)	0.024(4)	0	0.001(3)	0
X6	0.016(4)	0.014(4)	0.025(4)	0	0.006(3)	0
O _w 1	0.039(6)	0.048(7)	0.033(6)	0	0.007(4)	0
O _w 2	0.11(3)	0.09(3)	0.05(2)	−0.03(2)	0.01(2)	0
O _w 3	0.041(9)	0.07(1)	0.15(2)	0	0.02(1)	0

Table 5. Selected bond lengths (Å) in the crystal structure of shkatulkalite.

Nb–O1 ^{4,18}	1.980(6)	Si1–O1	1.603(6)	Na1–O _w 2 ^{9,18}	2.01(3)
Nb–O _w 1	2.29(1)	Si1–O2	1.634(4)	Na1–O3 ^{9,18}	2.641(7)
Nb–O3 ^{2,5}	1.979(6)	Si1–O3	1.612(6)	Na1–O1 ^{7,10}	2.650(7)
Nb–O5	1.770(8)	Si1–O4	1.615(6)	Na1–X6	2.67(1)
<Nb–O>	1.995	<Si–O>	1.616	Na1–O2 ^{7,18}	2.774(9)
				<Na1–X,O>	2.534
Ti–O4 ^{8,9,12,18}	1.996(5)	Na2–O4 ^{6,18}	2.282(5)		
Ti–X6 ^{4,18}	1.959(8)	Na2–X6 ^{2,8}	2.353(6)	Na3–O5 ^{13,18}	2.305(8)
<Ti–O,X>	1.984	Na2–O5 ^{1,18}	2.389(6)	Na3–O4 ^{1,2}	2.535(5)
		<Na2–O,X>	2.342	Na3–O4 ^{5,6}	2.535(5)
				<Na3–O>	2.458

¹ 1 − x, 2 − y, 1 − z; ² 1 + x, +y, +z; ³ 1 + x, 1 + y, +z; ⁴ +x, 2 − y, +z; ⁵ 1 + x, 2 − y, +z; ⁶ 1 − x, +y, 1 − z; ⁷ −1 + x, +y, +z; ⁸ −x, 1 − y, 1 − z; ⁹ +x, 1 − y, +z; ¹⁰ −1 + x, 1 − y, +z; ¹¹ −1 + x, −1 + y, +z; ¹² −x, +y, 1 − z; ¹³ 2 − x, 2 − y, 1 − z; ¹⁴ −1 − x, 1 − y, −z; ¹⁵ −x, 1 − y, −z; ¹⁶ −x, +y, −z; ¹⁷ −1 − x, −y, −z; ¹⁸ x, y, z.

Table 6. Bond-valence analysis (v.u. = valence units) for shkatulkalite.

Atom	Nb	Ti	Si	Na1	Na2	Na3	Total
O1	0.83↓ × 2		1.06	0.10			1.99
O2			0.97→ × 2	0.07, 0.08			2.09
O3	0.83↓ × 2		1.03	0.10↓ × 2			1.96
O4		0.61↓ × 4	1.03		0.27↓ × 2	0.14↓ × 4	2.05
O5	1.47				0.20↓→ × 2	0.26↓ × 2	2.13
X6		0.68↓ × 2		0.10	0.22↓→ × 2		1.22
O1w	0.36						0.36
O2w				0.56↓ × 2			0.56
Total	5.15	3.81	4.09	1.77	1.40	1.06	

3. Results

The crystal structure of shkatulkalite is based upon the HOH blocks consisting of one octahedral (O) sheet sandwiched between two heteropolyhedral (H) sheets (Figure 2a). According to Sokolova [17], the HOH blocks are of the type III with one Ti *apfu* present in the O sheet (Figure 2b). The blocks are parallel to (001) and are separated from each other (Figure 3a) with interlayer space occupied by Na1 atoms and H₂O groups. The Na2, Na3, and Ti sites are located within the O sheet. The H sheets are formed by NbO₆ octahedra and Si₂O₇ groups sharing common O atoms.

The *Na1* site is coordinated by eight anions (taking into account the disorder observed for the O_w2 site with adjacent O_w2 sites located at 1.318 Å) and is located approximately in the center of a six-membered ring in the *H* layer (Figure 4). The relatively high coordination number (8) and the long average $\langle Na1-O \rangle$ bond length of 2.534 Å indicate the capability of this site to accumulate large cations such as K^+ , Sr^{2+} and Ba^{2+} present in shkatulkalite. The structure refinement indicated the presence of rather short $Na1-O_w2$ contact of 2.01 Å, which we explain by the static disorder observed for both *Na1* and O_w2 sites (note also the high values of their atomic displacement parameters). The *Na2* and *Na3* sites are octahedrally coordinated by six anions each. The $Na2O_6$ octahedron is more compact, with the mean $\langle Na2-O \rangle$ bond length of 2.342 Å, the bond-valence sum (BVS) of 1.40 valence units (v.u.) and the site-scattering factor (SSF) of $12.54 e^-$ all pointing out that, in addition to Na^+ , this site also incorporates Ca^{2+} and Mn^{2+} cations (Table 3). The refinement of the SSF of the *Na3* site is consistent with its full occupancy by Na^+ cations, which is also confirmed by its BVS (1.06 v.u.) and the $\langle Na3-O \rangle$ bond length of 2.458 Å.

The *Nb* and *Ti* sites are both octahedrally coordinated by O atoms. The *Nb* site contains significant amount of Ti (its refined SSF corresponds to the composition $Nb_{0.75}Ti_{0.25}$). The NbO_6 octahedron is essentially distorted with one short (1.770 Å) $Nb-O5$ bond opposite to one long $Nb-O_w1$ (2.29 Å) bond, and four intermediate (~ 1.98 Å) $Nb-O$ bonds. This kind of octahedral distortion is typical for NbO_6 octahedra in *H* sheets and was observed, for instance, in vuonnemite, $Na_{11}TiNb_2(Si_2O_7)_2(PO_4)_2O_3F$ [35,36], and epistolite, $Na_4TiNb_2(Si_2O_7)_2O_2(OH)_2(H_2O)_4$ [37], two minerals most closely related to shkatulkalite (see below). The refined SSF of the *Ti* site is close to $22 e^-$, which would account for the full occupancy of this site by Ti. However, this would contradict the predominance of Nb over Ti observed in the chemical analyses (Table 1), which prompted us to suggest that the *Ti* site also accommodates Mn^{2+} cations present in shkatulkalite. It is rather common for divalent cations and, in particular, Mn^{2+} to substitute for Ti in the octahedral sites of the *O* sheet in heterophyllosilicates. Such a substitution was reported, for instance, for sobolevite, $Na_{13}Ca_2Mn_2Ti_3(Si_2O_7)_2(PO_4)_4O_3F_3$ [38,39].

The BVS for the X6 site in shkatulkalite is 1.22 v.u., which is compatible with its occupancy by $(OH)^-$ or F^- anions. The $(OH)_{0.82}F_{0.18}$ assigned to this site in Table 3 was calculated to conform with the results of the chemical analyses that demonstrate the presence in shkatulkalite of 0.36 F *apfu*.

The interlayer between the adjacent *HOH* blocks in shkatulkalite is occupied by a number of partially occupied O_w sites that belong to H_2O molecules. The O_w1 atom is bonded to the *Nb* site, forming a long apical Nb- H_2O bond in the NbO_6 octahedra. The O_w2 site is linked to the *Na1* site and is split into two sites, with the total occupancy of 68%. The O_w3-O_w8 sites are purely interlayer with the occupancies in the range from 19% to 92%. However, there are several H_2O positions that are mutually excluding (O_w4-O_w5 , O_w6-O_w7 , etc.). The maximum amount of H_2O in the formula considering all incompatible sites is 10 H_2O per formula unit. Therefore, the amount of H_2O molecules in the ideal formula can be written as *n*, where $n \leq 10$. It seems that the cohesion among different TS-blocks is ensured through hydrogen bonding between the H_2O molecule of the O_w1 site (apical anion of NbO_6 octahedra) and the H_2O molecule of the O_w8 site. However, no precise picture of the hydrogen bonding in shkatulkalite can be derived, owing to the high degree of disorder observed for the interlayer sites.

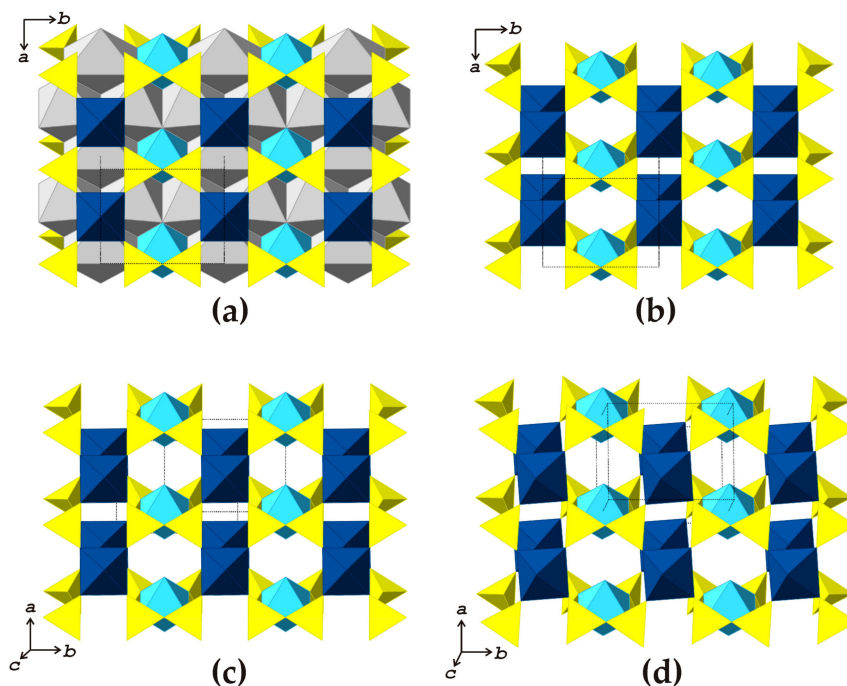


Figure 2. The HOH block in shkatulkalite (a); and the HOH blocks in shkatulkalite (b); epistolite (c) and vuonnemite (d) with the NaO₆ octahedra of the O sheets omitted for clarity. Legend: Nb, Ti, Na, and Si polyhedra are shown in dark-blue, light-blue, gray, and yellow colors, respectively.

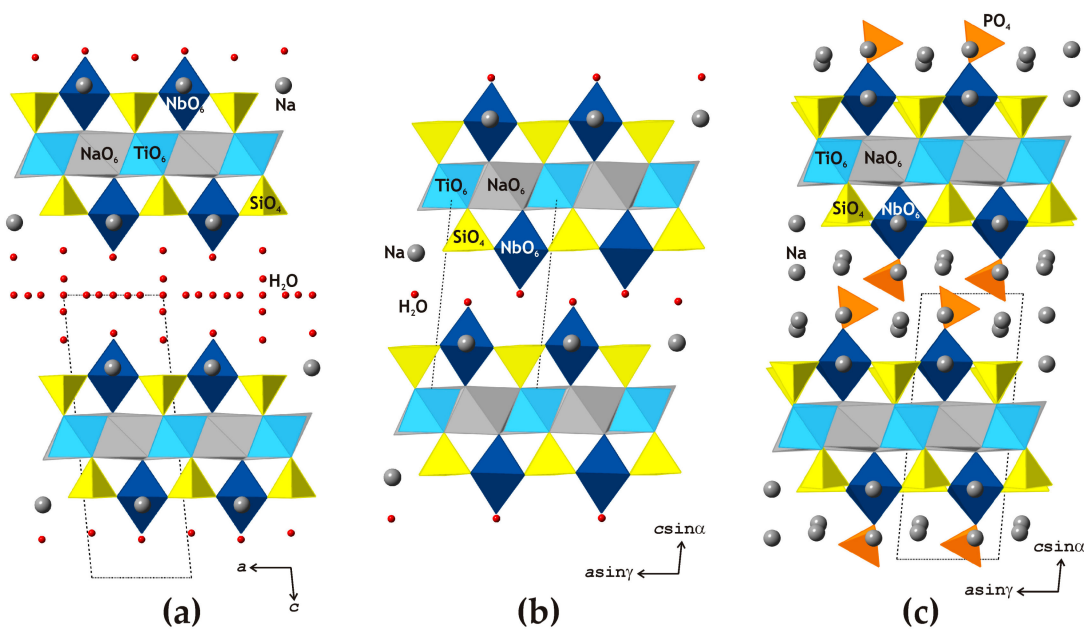


Figure 3. The crystal structures of shkatulkalite (a); epistolite (b) and vuonnemite (c) projected along the b axes. Legend: Nb, Ti, P, Na, and Si polyhedra are shown in dark-blue, light-blue, orange, gray and yellow colors, respectively. Interlayer Na and H₂O sites are shown as gray and red spheres, respectively.

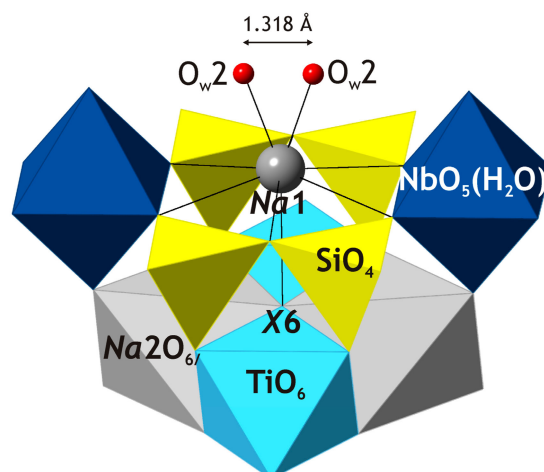


Figure 4. The local coordination environment of the *Na1* site in the crystal structure of shkatulkalite. Note that the *O_w2* sites are partially occupied (site occupation factor = 0.37). Legend as in Figure 3.

According to the crystal-structure refinement, the crystal-chemical formula of shkatulkalite can be written as $[\text{Na}_{3.94}\square_{0.50}\text{Sr}_{0.14}\text{Mn}_{0.14}\text{Ba}_{0.12}\text{Ca}_{0.12}\text{K}_{0.04}][\text{Nb}_{1.50}\text{Ti}_{1.27}\text{Mn}^{2+}_{0.20}\square_{0.03}][\text{Si}_2\text{O}_7]_2\text{O}_2[(\text{OH})_{0.82}\text{F}_{0.18}]_2 \cdot 7.43\text{H}_2\text{O}$, which is in very general agreement with the empirical chemical formula given above, taking into account the difficulties associated with the study of the mineral by the electron-microprobe analysis. It is noteworthy that, according to the chemical analyses, the H_2O content in shkatulkalite ranges from 4.32 to 6.67 apfu. Thus, by analogy to selivanovaite and murmanite [11,25] the interlayer H_2O content in shkatulkalite is variable and may be defined as $n\text{H}_2\text{O}$. Taking into account the cations prevalent at different atomic sites in shkatulkalite, its ideal chemical formula should be written as $\text{Na}_5\text{Nb}_2\text{Ti}[\text{Si}_2\text{O}_7]_2\text{O}_2(\text{OH})_2 \cdot n\text{H}_2\text{O}$, where $n \leq 10$, which is not electroneutral and contains one extra positive charge. Therefore, we assume that the incorporations of Ti into Nb and Mn into Ti sites are important for charge-balance considerations, and suggest the general formula should be written as $\text{Na}_5(\text{Nb}_{1-x}\text{Ti}_x)_2(\text{Ti}_{1-y}\text{Mn}^{2+y})[\text{Si}_2\text{O}_7]_2\text{O}_2(\text{OH})_2 \cdot n\text{H}_2\text{O}$, where $x + y = 0.5$, $n \leq 10$. For the sample of shkatulkalite under investigation $x \approx y \approx 0.25$. For the two critical cases of $x = 0.5$ or $y = 0.5$, the end-member formulae would be $\text{Na}_5(\text{NbTi})\text{Ti}[\text{Si}_2\text{O}_7]_2\text{O}_2(\text{OH})_2 \cdot n\text{H}_2\text{O}$ and $\text{Na}_5\text{Nb}_2(\text{Ti}_{0.5}\text{Mn}^{2+}_{0.5})[\text{Si}_2\text{O}_7]_2\text{O}_2(\text{OH})_2 \cdot n\text{H}_2\text{O}$ (or $\text{Na}_{10}\text{Nb}_4\text{TiMn}^{2+}[\text{Si}_2\text{O}_7]_4\text{O}_4(\text{OH})_4 \cdot n\text{H}_2\text{O}$), $n \leq 10$, respectively.

4. Discussion

The structure of shkatulkalite represents the basic structure type B5(GIII), according to Sokolova and Cámara [40] that was inferred by inverse prediction. In fact, Sokolova and Cámara [40] introduced the concept of basic and derivative structures for TS-block minerals and stated that a derivative structure is related to two or more basic structures of the same group. Hence a derivative structure can be built by adding basic structures *via* sharing the central O sheet of the TS blocks of adjacent structural fragments. The inverse prediction of the structure of shkatulkalite to B5(GIII) is now completely confirmed with the present results. Incidentally, the ideal formula of B5(GII) predicted by Sokolova and Cámara [40] is $\square_2\text{Nb}_2\text{Na}_2\text{M}^{2+}\text{Ti}(\text{Si}_2\text{O}_7)_2\text{O}_2(\text{OH})_2(\text{H}_2\text{O})_8$ (with $\text{M}^{2+} = \text{Mn}, \text{Ca}$), while the proposed ideal formula by us for shkatulkalite is $\text{Na}_5(\text{Nb}_{1-x}\text{Ti}_x)_2(\text{Ti}_{1-y}\text{Mn}^{2+y})[\text{Si}_2\text{O}_7]_2\text{O}_2(\text{OH})_2 \cdot n\text{H}_2\text{O}$, where $x + y = 0.5$ and $n \leq 10$, which is a remarkable agreement. It is worth noting that Cámara et al. [41] have already confirmed the right prediction of B7(GIV) structure type with the crystal structure of kolskyite.

In agreement with the suggestions by Németh et al. [25] and Sokolova and Cámara [6], shkatulkalite belongs to the seidozerite supergroup, since its structure is based upon the HOH [22] or TS [17] blocks. More precisely, shkatulkalite is a member of the lamprophyllite group, having $\text{Ti} + (\text{Nb} + \text{Mn}) = 3$ apfu, from which the H and O sheets has 2 and 1 ($\text{Ti} + \text{Nb} + \text{Mn}$) apfu, respectively. The

most closely related species to shkatulkalite are vuonnemite, $\text{Na}_{11}\text{TiNb}_2(\text{Si}_2\text{O}_7)_2(\text{PO}_4)_2\text{O}_3\text{F}$ [35,36], and epistolite, $\text{Na}_4\text{TiNb}_2(\text{Si}_2\text{O}_7)_2\text{O}_2(\text{OH})_2(\text{H}_2\text{O})_4$ [37,38], crystal structures of which are shown in Figure 3b,c, respectively. The three minerals are based upon the same topological type of the HOH blocks (Figure 2b–d) with different layer symmetries ($p2/m$ in shkatulkalite, and $p - 1$ in vuonnemite and epistolite). In all three minerals, the HOH blocks are parallel to (001), but the c parameters are different and equal to 15.573, 14.450 and 12.041 Å for shkatulkalite, vuonnemite and epistolite, respectively. In fact, both shkatulkalite and epistolite can be considered derivatives of vuonnemite and can be obtained from the latter at least through the *gedanken* experiment by removing the some Na^+ and all $(\text{PO}_4)^{3-}$ ions and subsequent hydration of the interlayer space. The hypothesis that shkatulkalite is a transformation mineral species that forms at the expense of vuonnemite (or some vuonnemite-related proto-mineral) seems quite reasonable, taking into account its high hydration state, which results in the very open packing of adjacent HOH blocks that is manifested in the large value of the c parameter and can be clearly seen in Figure 3a. In contrast, in the crystal structure of epistolite (Figure 3b), the packing of the HOH blocks is quite dense, resulting in the shrinkage of the c parameter. The syntactic intergrowths of shkatulkalite and epistolite reported by Németh et al. [25] may point out to the following growth scenarios: (1) both minerals are primary phases that crystallize simultaneously; (2) both minerals are transformation species that form according to the sequence “vuonnemite (or vuonnemite-related proto-mineral) \rightarrow shkatulkalite \rightarrow epistolite”; or (3) both minerals are transformation species that form along two different pathways, “vuonnemite \rightarrow shkatulkalite” and “vuonnemite \rightarrow epistolite”. The reported observations of pseudomorphs of shkatulkalite after vuonnemite suggest that, at least in some environments, shkatulkalite is indeed a transformation mineral species that inherits basic structural features from vuonnemite in accordance with Khomyakov’s structural inheritance principle [42]. The secondary nature and the status of shkatulkalite as a transformation mineral species may also account for the difficulties encountered when investigating the mineral by means of electron microprobe and crystal-structure analysis. The absence of precise agreement between the chemical and structural studies (the obvious cation deficiency observed in three series of independent chemical analyses and in the original report [23]) remains an issue that we cannot resolve at the present time.

Author Contributions: Conceptualization, A.A.Z., E.A.S. and S.V.K.; Methodology, A.A.Z. and T.L.P.; Investigation, A.A.Z., E.A.S., Y.E.S., T.L.P., L.M.L., L.A.P., and V.N.Y.; Writing-Original Draft Preparation, A.A.Z.; Writing-Review & Editing, S.V.K.; Visualization, S.V.K.

Funding: This research was funded by the President of Russian Federation grant for leading scientific schools (project NSh-3079.2018.5) and Russian Foundation for Basic Research (grant 16-05-00427).

Acknowledgments: The X-ray diffraction studies were performed in the X-ray Diffraction Resource Centre of St. Petersburg State University. The chemical analytical studies were done in “Geomodel” Resource Centre of St. Petersburg State University and Geological Institute, Kola Science Centre, Russian Academy of Sciences.

Conflicts of Interest: The authors declare no conflict of interest.

References

1. Rocha, J.; Anderson, M.W. Microporous titanosilicates and other novel mixed octahedral–tetrahedral framework oxides. *Eur. J. Inorg. Chem.* **2000**, *2000*, 801–818. [[CrossRef](#)]
2. Noh, Y.D.; Komarneni, S.; Mackenzie, K.J.D. Titanosilicates: Giant exchange capacity and selectivity for Sr and Ba. *Sep. Purif. Technol.* **2012**, *95*, 222–226. [[CrossRef](#)]
3. Oleksienko, O.; Wolkersdorfer, C.; Sillanpaa, M. Titanosilicates in cation adsorption and cation exchange—A review. *Chem. Eng. J.* **2017**, *317*, 570–585. [[CrossRef](#)]
4. Hu, J.; Ma, Z.; Sa, R.; Zhang, Y.; Wu, K. Theoretical perspectives on the structure, electronic, and optical properties of titanosilicates $\text{Li}_2\text{M}_4[(\text{TiO})\text{Si}_4\text{O}_{12}]$ ($\text{M} = \text{K}^+, \text{Rb}^+$). *Phys. Chem. Chem. Phys.* **2017**, *19*, 15120–15128. [[CrossRef](#)] [[PubMed](#)]
5. Prech, J. Catalytic performance of advanced titanosilicate selective oxidation catalysts—A review. *Catal. Rev. Sci. Eng.* **2018**, *60*, 71–131. [[CrossRef](#)]

6. Sokolova, E.; Cámara, F. The seidozerite supergroup of TS-block minerals: Nomenclature and classification, with change of the following names: Rinkite to rinkite-(Ce), mosandrite to mosandrite-(Ce), hainite to hainite-(Y) and innelite-1T to innelite-1A. *Mineral. Mag.* **2017**, *81*, 1457–1484. [[CrossRef](#)]
7. Sokolova, E.; Cámara, F.; Abdu, Y.A.; Hawthorne, F.C.; Horváth, P.; Pfenninger-Horváth, E. Bobshannonite, $\text{Na}_2\text{KBa}(\text{Mn},\text{Na})_8(\text{Nb},\text{Ti})_4(\text{Si}_2\text{O}_7)_4\text{O}_4(\text{OH})_4(\text{O},\text{F})_2$, a new TS-block mineral from Mont Saint-Hilaire, Québec, Canada: Description and crystal structure. *Mineral. Mag.* **2015**, *79*, 1791–1811. [[CrossRef](#)]
8. Lykova, I.S.; Pekov, I.V.; Chukanov, N.V.; Belakovskiy, D.I.; Yapaskurt, V.O.; Zubkova, N.V.; Britvin, S.N.; Giester, G. Calciomurmanite, $(\text{Na},\text{vac})_2\text{Ca}(\text{Ti},\text{Mg},\text{Nb})_4[\text{Si}_2\text{O}_7]_2\text{O}_2(\text{OH},\text{O})_2(\text{H}_2\text{O})_4$, a new mineral from the Lovozero and Khibiny alkaline complexes, Kola Peninsula, Russia. *Eur. J. Mineral.* **2016**, *28*, 835–845. [[CrossRef](#)]
9. Lyalina, L.M.; Zolotarev, A.A., Jr.; Selivanova, E.A.; Savchenko, Y.E.; Krivovichev, S.V.; Mikhailova, Y.A.; Kadyrova, G.I.; Zozulya, D.R. Batievaite-(Y), $\text{Y}_2\text{Ca}_2\text{Ti}[\text{Si}_2\text{O}_7]_2(\text{OH})_2(\text{H}_2\text{O})_4$, a new mineral from nepheline syenite pegmatite in the Sakharjok massif, Kola Peninsula, Russia. *Mineral. Petrol.* **2016**, *110*, 895–904. [[CrossRef](#)]
10. Sokolova, E.; Cámara, F.; Hawthorne, F.C.; Semenov, E.I.; Ciriotti, M.E. Lobanovite, $\text{K}_2\text{Na}(\text{Fe}^{2+}_4\text{Mg}_2\text{Na})\text{Ti}_2(\text{Si}_4\text{O}_{12})_2\text{O}_2(\text{OH})_4$, a new mineral of the astrophyllite supergroup and its relation to magnesioastrophyllite. *Mineral. Mag.* **2017**, *81*, 175–181. [[CrossRef](#)]
11. Pakhomovsky, Y.A.; Panikorovskii, T.L.; Yakovenchuk, V.N.; Ivanyuk, G.Y.; Mikhailova, J.A.; Krivovichev, S.V.; Bocharov, V.N.; Kalashnikov, A.O. Selivanovaite, $\text{NaTi}_3(\text{Ti},\text{Na},\text{Fe},\text{Mn})_4[(\text{Si}_2\text{O}_7)_2\text{O}_4(\text{OH},\text{H}_2\text{O})_4] \cdot n\text{H}_2\text{O}$, a new rock-forming mineral from the eudialyte-rich malignite of the Lovozero alkaline massif (Kola Peninsula, Russia). *Eur. J. Mineral.* **2018**, *30*. [[CrossRef](#)]
12. Cámara, F.; Sokolova, E.; Abdu, Y.A.; Hawthorne, F.C.; Charrier, T.; Dorcet, V.; Carpentier, J.-F. Fogoite-(Y), $\text{Na}_3\text{Ca}_2\text{Y}_2\text{Ti}(\text{Si}_2\text{O}_7)_2\text{OF}_3$, a Group I TS-block mineral from the Lagoa do Fogo, the Fogo volcano, São Miguel Island, the Azores: Description and crystal structure. *Mineral. Mag.* **2017**, *81*, 369–381. [[CrossRef](#)]
13. Andrade, M.B.; Yang, H.; Downs, R.T.; Färber, G.; Contreira Filho, R.R.; Evans, S.H.; Loehn, C.W.; Schumer, B.N. Fluorlamprophyllite, $\text{Na}_3(\text{SrNa})\text{Ti}_3(\text{Si}_2\text{O}_7)_2\text{O}_2\text{F}_2$, a new mineral from Poços de Caldas alkaline massif, Morro do Serrote, Minas Gerais, Brazil. *Mineral. Mag.* **2018**, *82*, 121–131. [[CrossRef](#)]
14. Belov, N.V.; Organova, N.I. Crystal chemistry and mineralogy of the lomonosovite group in the light of the crystal structure of lomonosovite. *Geokhimiya* **1962**, *1*, 4–13.
15. Belov, N.V. *Essays on Structural Mineralogy*; Nedra: Moscow, Russia, 1976; 344p. (In Russian)
16. Pyatenko, Y.A.; Voronkov, A.A.; Pudovkina, Z.V. *Mineralogical Crystal Chemistry of Titanium*; Nauka: Moscow, Russia, 1976; 155p. (In Russian)
17. Sokolova, E. From structure topology to chemical composition. I. Structural hierarchy and stereochemistry in titanium disilicate minerals. *Can. Mineral.* **2006**, *44*, 1273–1330. [[CrossRef](#)]
18. Egorov-Tismenko, Y.K.; Sokolova, E.V. Comparative crystal chemistry of a group of titanium silicate analogues of mica. In *Comparative Crystal Chemistry*; Moscow State University: Moscow, Russia, 1987; pp. 96–106. (In Russian)
19. Egorov-Tismenko, Y.K.; Sokolova, E.V. Homologous series seidozerite-nacaphite. *Mineral. ZH* **1990**, *12*, 40–49. (In Russian)
20. Ferraris, G. Polysomatism as a tool for correlating properties and structure. In *Modular Aspects of Minerals*; Merlino, S., Ed.; Eötvös University Press: Budapest, Hungary, 1997; pp. 275–295.
21. Ferraris, G. Modular structures—The paradigmatic case of heterophyllosilicates. *Z. Kristallogr.* **2008**, *223*, 76–84. [[CrossRef](#)]
22. Ferraris, G.; Ivaldi, G.; Khomyakov, A.P.; Soboleva, S.V.; Belluso, E.; Pavese, A. Nafertisite, a layer titanosilicate member of a polysomatic series including mica. *Eur. J. Mineral.* **1996**, *8*, 241–249. [[CrossRef](#)]
23. Menshikov, Y.P.; Khomyakov, A.P.; Polezhaeva, L.I.; Rastsvetaeva, R.K. Shkatulkalite- $\text{Na}_{10}\text{MnTi}_3\text{Nb}_3(\text{Si}_2\text{O}_7)_6(\text{OH})_2\text{F} \cdot 12\text{H}_2\text{O}$ a new mineral. *Zap. Vseross. Mineral. Obs.* **1996**, *125*, 120–126. (In Russian)
24. Sokolova, E.; Cámara, F. From structure topology to chemical composition. XXI. Understanding the crystal chemistry of barium in TS-block minerals. *Can. Mineral.* **2016**, *54*, 79–95. [[CrossRef](#)]
25. Németh, P.; Ferraris, G.; Radnóczy, G.; Ageeva, O.A. TEM and X-ray study of syntactic intergrowths of epistolite, murmanite and shkatulkalite. *Can. Mineral.* **2005**, *43*, 973–987. [[CrossRef](#)]
26. Horvath, L.; Pfenninger-Horvath, E.; Gault, R.A.; Tarasoff, P. Mineralogy of the Saint-Amable Sill, Varennes and Saint-Amable, Quebec. *Miner. Rec.* **1998**, *29*, 83–118.

27. Khomyakov, A.P. Transformation mineral species and their use in paleomineralogical reconstructions. In Proceedings of the 30th International Geological Congress, Beijing, China, 4–14 August 1996; p. 450.
28. Khomyakov, A.P. The largest source of minerals with unique structure and properties. In *Minerals as Advanced Materials I*; Krivovichev, S.V., Ed.; Springer: Heidelberg/Berlin, Germany, 2008; pp. 71–77, ISBN 978-3-540-77123-4.
29. Pekov, I.V. *Lovozero Massif: History, Pegmatites, Minerals*; Ocean Press: Moscow, Russia, 2000; ISBN 978-5900395272.
30. Bruker-AXS. *APEX2*, Version 2014.11-0; Bruker-AXS: Madison, WI, USA, 2014.
31. Sheldrick, G.M. *SADABS*, University of Goettingen: Goettingen, Germany, 2007.
32. Sheldrick, G.M. Crystal structure refinement with *SHELXL*. *Acta Crystallogr.* **2015**, *C71*, 3–8.
33. Dolomanov, O.V.; Bourhis, L.J.; Gildea, R.J.; Howard, J.A.K.; Puschmann, H. Olex2: A complete structure solution, refinement and analysis program. *J. Appl. Crystallogr.* **2009**, *42*, 339–341. [[CrossRef](#)]
34. Brese, N.E.; O’Keeffe, M. Bond-valence parameters for solids. *Acta Crystallogr.* **1991**, *B47*, 192–197. [[CrossRef](#)]
35. Bussen, I.V.; Denisov, A.P.; Zabavnikova, N.I.; Kozyreva, L.V.; Menshikov, Y.P.; Lipatova, E.A. Vuonnemite, a new mineral. *Zap. Vseross. Mineral. Obs.* **1973**, *102*, 423–426. (In Russian) [[CrossRef](#)]
36. Ercit, T.S.; Cooper, M.A.; Hawthorne, F.C. The crystal structure of vuonnemite, $\text{Na}_{11}\text{Ti}^{4+}\text{Nb}_2(\text{Si}_2\text{O}_7)_2(\text{PO}_4)_2\text{O}_3(\text{F,OH})$, a phosphate-bearing sorosilicate of the lomonosovite group. *Can. Mineral.* **1998**, *37*, 1311–1320.
37. Sokolova, E.; Hawthorne, F.C. The crystal chemistry of epistolite. *Can. Mineral.* **2004**, *42*, 797–806. [[CrossRef](#)]
38. Khomyakov, A.P.; Kurova, T.A.; Chistyakova, N.I. Sobolevite $\text{Na}_{14}\text{Ca}_2\text{MnTi}_3\text{P}_4\text{Si}_4\text{O}_{34}$ —A new mineral. *Zap. Vseross. Mineral. Obs.* **1983**, *112*, 456–461. (In Russian)
39. Sokolova, E.; Hawthorne, F.C.; Khomyakov, A.P. Polyphite and sobolevite: Revision of their crystal structures. *Can. Mineral.* **2005**, *43*, 1527–1544. [[CrossRef](#)]
40. Sokolova, E.; Cámara, F. From structure topology to chemical composition. XVI. New developments in the crystal chemistry and prediction of new structure topologies for titanium disilicate minerals with the TS block. *Can. Mineral.* **2013**, *51*, 861–891. [[CrossRef](#)]
41. Cámara, F.; Sokolova, E.; Abdu, Y.A.; Hawthorne, F.C.; Khomyakov, A.P. Kolskyite, $(\text{Ca}\square)\text{Na}_2\text{Ti}_4(\text{Si}_2\text{O}_7)_2\text{O}_4(\text{H}_2\text{O})_7$, a Group-IV Ti-disilicate mineral from the Khibiny alkaline massif, Kola Peninsula, Russia: Description and crystal structure. *Can. Mineral.* **2013**, *51*, 921. [[CrossRef](#)]
42. Khomyakov, A.P.; Yushkin, N.P. The principle of inheritance in crystallogenesis. *Dokl. Akad. Nauk SSSR* **1981**, *256*, 1229–1233.



© 2018 by the authors. Licensee MDPI, Basel, Switzerland. This article is an open access article distributed under the terms and conditions of the Creative Commons Attribution (CC BY) license (<http://creativecommons.org/licenses/by/4.0/>).